iScience

Article

mtDNA extramitochondrial replication mediates mitochondrial defect effects

Zhaoliang Shan,
Shengnan Li,
Yuxue Gao, ...,
Guochun Zhao,
Yan Wang, Qing
Zhang

wangyan4127@bjhmoh.cn
(Y.W.)
zhangqing@nju.edu.cn (Q.Z.)

Highlights

Med8/Tfb4-mtSSB/PolG2/
mtDNA-helicase axis
mediates mitochondrial
defect effects

The above axis drives
mtDNA extramitochondrial
replication

Cytosolic mtDNA
replication triggers innate
immune response to
mediate the effects

Med8/Tfb4-mtSSB/PolG2/
mtDNA-helicase axis also
modulates *Drosophila*
lifespan

Article

mtDNA extramitochondrial replication mediates mitochondrial defect effects

Zhaoliang Shan,[1,3] Shengnan Li,[1,3] Yuxue Gao,[1,3] Chunhua Jian,[1] Xiuxiu Ti,[1] Hui Zuo,[1] Ying Wang,[1] Guochun Zhao,[1] Yan Wang,[2,*] and Qing Zhang[1,4,*]

SUMMARY

A high ratio of severe mitochondrial defects causes multiple human mitochondrial diseases. However, until now, the *in vivo* rescue signal of such mitochondrial defect effects has not been clear. Here, we built fly mitochondrial defect models by knocking down the essential mitochondrial genes *dMterf4* and *dMrps23*. Following genome-wide RNAi screens, we found that knockdown of *Med8/Tfb4/mtSSB/PolG2/mtDNA-helicase* rescued *dMterf4/dMrps23* RNAi-mediated mitochondrial defect effects. Extremely surprisingly, they drove mtDNA replication outside mitochondria through the Med8/Tfb4-mtSSB/PolG2/mtDNA-helicase axis to amplify cytosolic mtDNA, leading to activation of the cGAS-Sting-like IMD pathway to partially mediate *dMterf4/dMrps23* RNAi-triggered effects. Moreover, we found that the Med8/Tfb4-mtSSB/PolG2/mtDNA-helicase axis also mediated other fly mitochondrial gene defect-triggered dysfunctions and *Drosophila* aging. Overall, our study demarcates the Med8/Tfb4-mtSSB/PolG2/mtDNA-helicase axis as a candidate mechanism to mediate mitochondrial defect effects through driving mtDNA extramitochondrial replication; dysfunction of this axis might be used for potential treatments for many mitochondrial and age-related diseases.

INTRODUCTION

Mitochondria are central to energy production and metabolic processes[1–3] and are made up of functionally distinct outer mitochondrial membrane (OMM) and inner mitochondrial membrane (IMM) that encapsulate the intermembrane space and matrix compartments.[4] In the matrix, the mitochondrial genome (mtDNA) is organized into discrete nucleoids and encodes critical proteins for the assembly and activity of mitochondrial respiratory complexes.[5,6] Mitochondria are dynamic and undergo continuous fission and fusion to retain a suitable morphology.[7,8] These properties confer widespread benefits on mitochondria, including efficient transport, increased homogenization of the mitochondrial population and efficient oxidative phosphorylation, all of which are critical for their optimal function in energy generation.

Mammalian mtDNA encodes 37 genes (including 13 protein coding subunits of the OXPHOS, 22 tRNAs and 2 rRNAs),[9,10] whereas the vast majority of the factors needed for mitochondrial function are encoded by the nucleus, thus underlining the need to coregulate the two genomes.[11,12] mtDNA replication is strongly dependent on nuclear-encoded factors, including mitochondrial single-strand DNA-binding protein (mtSSB), mtDNA polymerase (POLγ), TWINKLE DNA helicase[13–16] and mitochondrial RNA polymerase (POLRMT), which correspond to *Drosophila* mtSSB, PolG2, mtDNA-helicase and PolrMT, respectively. They form the minimal mitochondrial replisome to coordinately direct mtDNA replication.[17] Among them, TWINKLE catalyzes the unwinding of double-strand mtDNA at the fork to release single-stranded DNA, which is stabilized, protected by mtSSB and subsequently used by POLγ as a template for mtDNA synthesis. POLRMT is essential for generating RNA primers for mtDNA replication.[18,19]

Dysfunction of multiple mitochondrial genes may impair mitochondrial integrity, leading to mtDNA release into the cytosol or outside cells.[20] As reported, Bax/Bak, mitochondrial porin voltage-dependent anion-selective channel (VDAC) and the mitochondrial permeability transition pore (mPTP) are involved in mediating mtDNA cytosolic release.[21–25] Later, the released cytosolic mtDNA can interact with cGAS and Toll-like reporter 9 to activate immune and inflammatory signaling pathways.[26–29] In addition, other kinds of mitochondrial impairment-initiated retrograde signals include the mitochondrial unfolded protein response (mtUPR), mitophagy and apoptosis.[30,31]

A high ratio of mitochondria with severe impairment will cause multiple human mitochondrial diseases including neurodegeneration and cancer.[32,33] However, until now, the *in vivo* rescue signal of such a mitochondrial defect effect has not been clear. Therefore, the

[1]State Key Laboratory of Pharmaceutical Biotechnology and MOE Key Laboratory of Model Animals for Disease Study, Jiangsu Key Laboratory of Molecular Medicine, Model Animal Research Center, School of Medicine, Nanjing University, Nanjing 210061, China
[2]Department of Cardiovascular Medicine, Beijing Hospital, National Center of Gerontology, Institute of Geriatric Medicine, Chinese Academy of Medical Sciences, Beijing, China
[3]These authors contributed equally
[4]Lead contact
*Correspondence: wangyan4127@bjmoh.cn (Y.W.), zhangqing@nju.edu.cn (Q.Z.)
https://doi.org/10.1016/j.isci.2024.108970

corresponding treatments for mitochondrial defect-initiated diseases are very limited. Here, to address this question, we built fly mitochondrial defect models by knocking down the essential mitochondrial genes *dMterf4* and *dMrps23*. Following genome-wide RNAi screens, we found that knockdown of *Med8/Tfb4/mtSSB/PolG2/mtDNA-helicase* rescued *dMterf4/dMrps23* RNAi-mediated mitochondrial defect effects. Unexpectedly and extremely surprisingly, they drove mtDNA replication outside mitochondria through the Med8/Tfb4-mtSSB/PolG2/mtDNA-helicase axis to accumulate cytosolic mtDNA, leading to activation of the cGAS-Sting-like IMD pathway to partially mediate *dMterf4/dMrps23* RNAi-triggered effects. Moreover, except for *dMterf4* and *dMrps23*, we found that the Med8/Tfb4-mtSSB/PolG2/mtDNA-helicase axis also mediated other fly mitochondrial gene defect-triggered dysfunctions, indicating that this axis may play a broader common role in mediating mitochondrial defect effects. Finally, we demonstrated that this axis was also involved in *Drosophila* aging.

RESULTS

Constructing *Drosophila* mitochondrial defect models through knockdown of *dMterf4* and *dMrps23*

Drosophila is a powerful system to conduct *in vivo* genome-wide screens to identify the rescue signal of mitochondrial defects, which is helpful to address the underlying mechanisms of mitochondrial diseases.[34] To find a possible common rescue signal, we built two mitochondrial defect models by knocking down the mitochondrial essential genes *dMterf4* (CG15390) and *dMrps23* (CG31842) with muscle specific Mef2-Gal4 to drive UAS-RNAis expression. dMterf4 is predicted to be involved in the regulation of mtDNA-templated transcription. While dMrps23 is involved in mitochondrial translation, dysfunction of the human homolog MRPS23 causes mitochondrial disease, named combined oxidative phosphorylation deficiency 46.[35,36] Taking *dMterf4* as an example, we found that its knockdown led to mitochondrial defects, as indicated by abnormal mitochondrial morphology, decreased ATP levels, impaired locomotion, abnormal erect or dropped wing postures and shortened lifespan at 25°C (Figures 1A–1G). When enhancing the expression of *dMterf4* RNAi by raising the temperature to 29°C, we observed that knockdown of *dMterf4* led to death (Figure 1H). To exclude the possible off-target effect of *dMterf4* RNAi, we coexpressed it with HA-dMterf4 and its human homolog MTERF4 transgenes, and found that both rescued the abnormal wing postures (Figure 1I), indicating that no off-target effect occurs and that MTERF4 is functionally conserved. Similarly, as shown in Figure S1, knockdown of *dMrps23* led to mitochondrial defects, and the function of MRPS23 is also evolutionarily conserved. Overall, these results strongly suggest that knockdown of *dMterf4* and *dMrps23* results in mitochondrial defects and that both *dMterf4* and *dMrps23* knockdown flies can be used as mitochondrial defect models.

Identifying a common Med8/Tfb4-mtSSB/PolG2/mtDNA-helicase axis that mediates *dMterf4/dMrps23* RNAi-triggered adverse effects

To systematically identify the *in vivo* rescue signal of *dMterf4* and *dMrps23* RNAis, we carried out genome-wide RNAi screens of conserved genes between flies and mammals and found that knockdown of *Med8*, *Tfb4*, *mtSSB*, *PolG2* and *mtDNA-helicase* could largely rescue both *dMterf4* and *dMrps23* RNAis-mediated abnormal wing posture phenotypes, indicating that they are common hits for mediating *dMterf4* and *dMrps23* RNAis-triggered adverse effects (Figures 2A, S2, and S3A).

To make the following experiments simple, next, we only focused on *dMterf4* due to its RNAi mediating a slightly stronger phenotype. We found that in addition to rescuing the abnormal wing phenotypes, knockdown of *Med8*, *Tfb4*, *mtSSB*, *PolG2* and *mtDNA-helicase* largely rescued motor impairment, decreased ATP levels, abnormal mitochondrial morphology, shortened lifespan at 25°C and death at 29°C (Figures 2B–2L). These observations indicate that mitochondrial defect effects mediated by *dMterf4* RNAi are suppressed by knockdown of *Med8*, *Tfb4*, *mtSSB*, *PolG2* and *mtDNA-helicase*.

As knockdown of *Med8*, *Tfb4*, *mtSSB*, *PolG2* and *mtDNA-helicase* suppressed *dMterf4* RNAi-mediated adverse effects, we investigated whether knockdown of *dMterf4* affects their expression. The results showed that knockdown of *dMterf4* upregulated their mRNA levels (Figure 2M) and promoted Tfb4 translocation into the nucleus in fly muscle (Figures 2N–2O''' and S4A–S4E'''). In addition, knockdown of any *Med8*, *Tfb4*, *mtSSB*, *PolG2*, and *mtDNA-helicase* gave a similar phenotype, implying that they may function in a linear way. Med8 is a member of the mediator complex, and Tfb4 belongs to the general transcription factor TFIIH family.[37,38] Usually, the mediator complex couples the gene-specific transcription factor and the general transcription factors/RNA polymerase II complex to regulate target gene transcription. Consistently, we found that Med8 bound to Tfb4 (Figure 2P). Next, when further testing whether Med8/Tfb4 regulates the transcription of *mtSSB*, *PolG2* and *mtDNA-helicase* in the *dMterf4* RNAi background, we found that knockdown of *Med8* and *Tfb4* reversed the *dMterf4* RNAi-mediated upregulation of *mtSSB*, *PolG2* and *mtDNA-helicase* mRNA levels (Figure 2Q). Collectively, these observations indicate that knockdown of *dMterf4* can upregulate *Med8* and *Tfb4* transcription and promote Tfb4 nuclear localization, which facilitates Med8/Tfb4 formation of a transcriptional complex to regulate the transcription of *mtSSB*, *PolG2* and *mtDNA-helicase*, suggesting that mitochondrial defect effects mediated by *dMterf4* RNAi are achieved through Med8/Tfb4 to the mtSSB/PolG2/mtDNA-helicase axis.

Importantly, except for rescue of *dMterf4* and *dMrps23* RNAis-mediated phenotypes, knockdown of *Med8*, *Tfb4*, *mtSSB*, *PolG2*, and *mtDNA-helicase* could also suppress the death caused by knockdown of other fly mitochondrial genes such as *mRpL13*, *mRpL22* and *mRpL52* (Figures S3B–S3D), indicating that the Med8/Tfb4-mtSSB/PolG2/mtDNA-helicase axis may play a broader common role in mediating many mitochondrial gene-triggered dysfunctions in *Drosophila*.
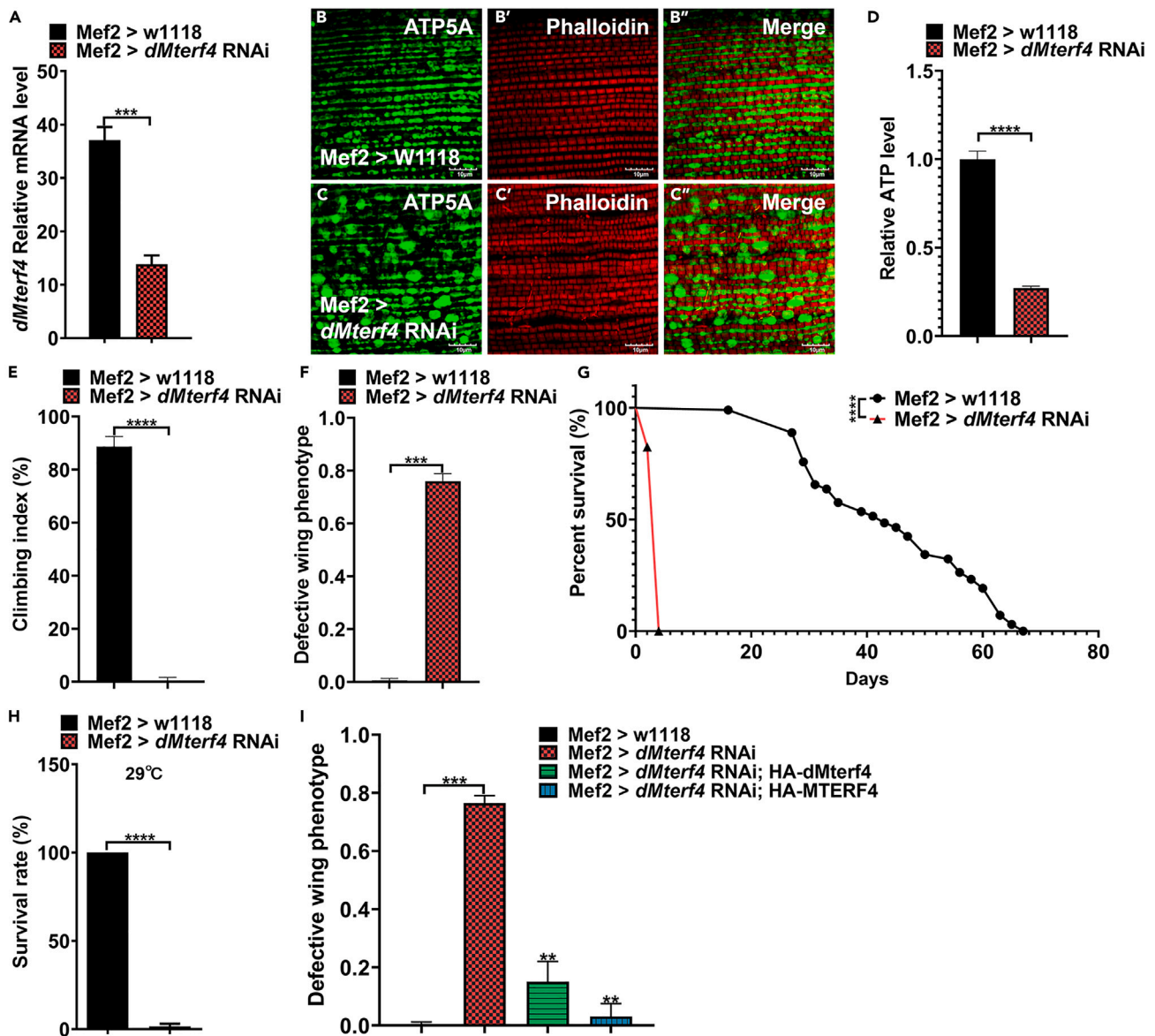
Figure 1. Constructing a *Drosophila* mitochondrial defect model through knockdown of *dMterf4*

(A) Knockdown of *dMterf4* decreased its mRNA level.

(B–G) Knockdown of *dMterf4* led to abnormal mitochondrial morphology (B-C″), decreased ATP level (D), reduced the climbing ability (E), defective wing postures (F) and shortened lifespan at 25°C (G). ATP5A (green) and phalloidin (red) staining were used to mark mitochondria and muscle actin fibers, respectively.

(H) Knockdown of *dMterf4* caused fly death at 29°C.

(I) Overexpression of HA-dMterf4 or its human homolog HA-MTERF4 rescued *dMterf4* RNAi-mediated abnormal wing postures. Data are represented as mean ± SD, asterisks indicate statistically significant difference. Scale bar, 10um.

The Med8/Tfb4-mtSSB/PolG2/mtDNA-helicase axis drives cytosolic mtDNA replication to mediate *dMterf4* RNAi-initiated adverse effects

The Med8/Tfb4-mtSSB/PolG2/mtDNA-helicase axis mediated the adverse effects of *dMterf4* RNAi, and knockdown of any mtDNA replication-needed *mtSSB*, *PolG2* and *mtDNA-helicase* largely rescued *dMterf4* RNAi-mediated phenotypes, implying that they function as functional units to mediate adverse effects by regulating mtDNA replication.

Given that knockdown of *dMterf4* hindered mtSSB, PolG2 and mtDNA-helicase into the mitochondrial matrix and promoted their cytosolic accumulation (including in the cytosol and outside of the OMM) (Figures 3A–3C), we next tested whether cytosolic accumulation of mtSSB, PolG2 and mtDNA-helicase can mediate the adverse effects. To do that, we made cytosolic localized forms of mtSSB, PolG2 and mtDNA-helicase, named mtSSBΔ1-47-3xHA, Tom20(1–50)-PolG2Δ1-20-3xHA and Tom20(1–50)-mtDNA-helicaseΔ1-33-3xHA, respectively. Among
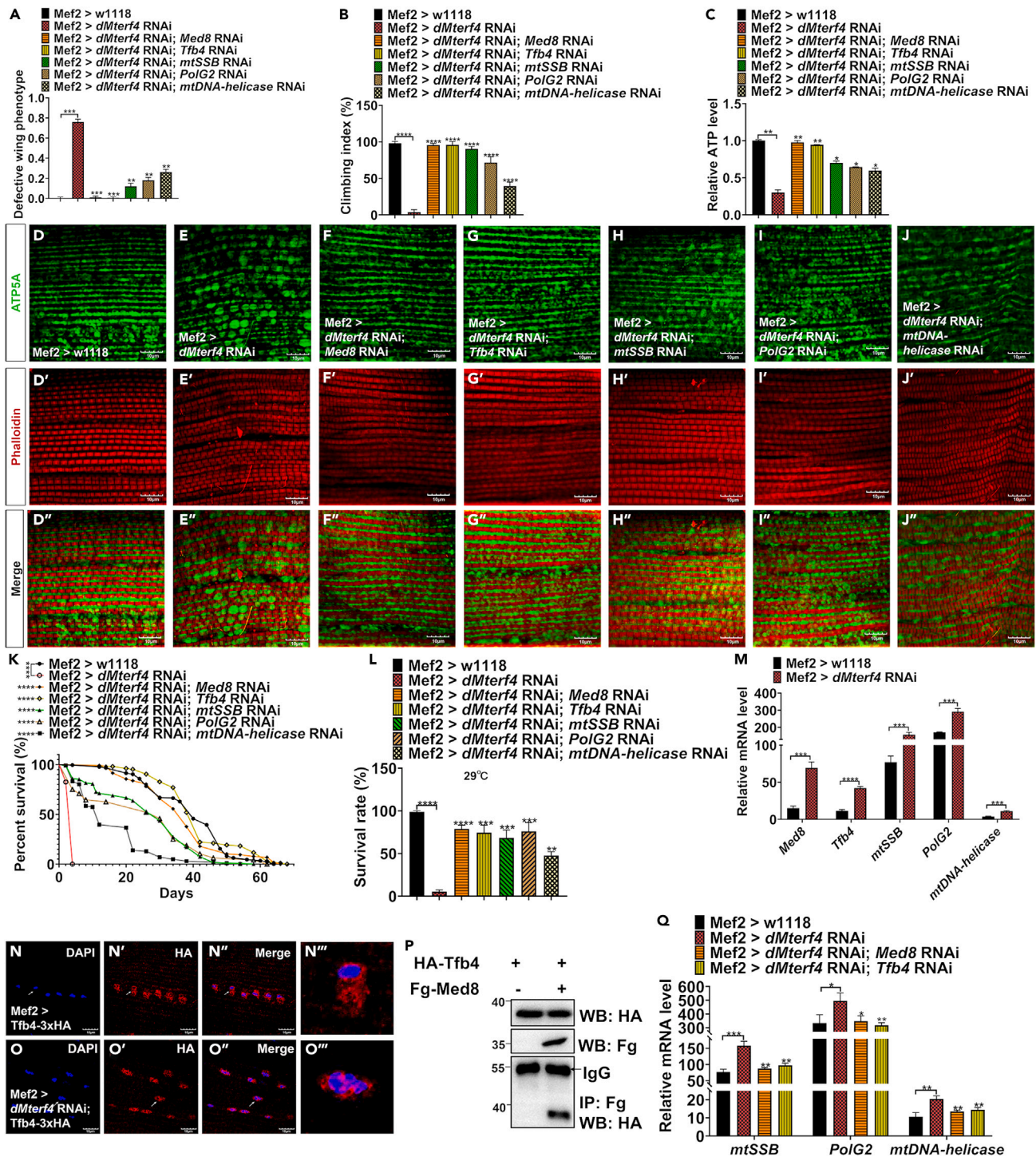
Figure 2. Identifying the Med8/Tfb4-mtSSB/PolG2/mtDNA-helicase axis that mediates *dMterf4* RNAi-triggered adverse effects

(A) Knockdown of *Med8*, *Tfb4*, *mtSSB*, *PolG2*, and *mtDNA-helicase* largely rescued the defective wing postures.

(B–L) Knockdown of *Med8*, *Tfb4*, *mtSSB*, *PolG2*, and *mtDNA-helicase* largely rescued motor impairment (B), decreased ATP level (C), abnormal mitochondrial morphology (D–J''), shortened lifespan at 25°C (K) and death under 29°C (L).

(M–O''') Knockdown of *dMterf4* increased the mRNA levels of *Med8*, *Tfb4*, *mtSSB*, *PolG2* and *mtDNA-helicase* (M), and promoted Tfb4 translocation into the nucleus in flies (N–O''').

(P) Fg-Med8 bound with HA-Tfb4.

(Q) Knockdown of *Med8* and *Tfb4* reversed the upregulated mRNA levels of *mtSSB*, *PolG2* and *mtDNA-helicase* in *dMterf4* knockdown flies. Data are represented as mean ± SD, asterisks indicate statistically significant difference. Scale bar, 10um.
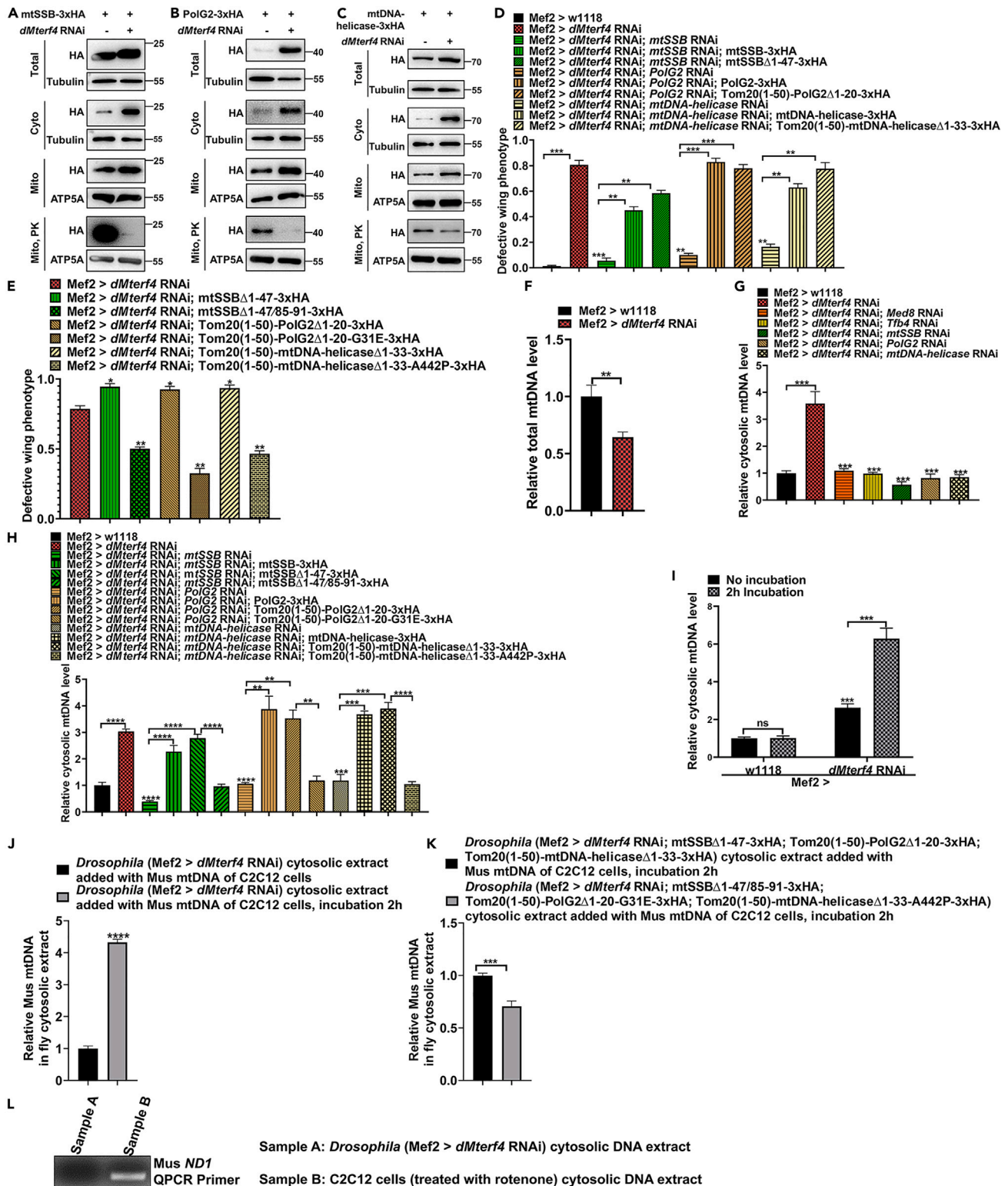
Figure 3. The Med8/Tfb4-mtSSB/PolG2/mtDNA-helicase axis drives cytosolic mtDNA replication to mediate *dMterf4* RNAi-initiated adverse effects

(A–C) Knockdown of *dMterf4* increased mtSSB, PolG2 and mtDNA-helicase accumulation in the cytosol and outside of the OMM. The mitochondria treated with or without proteinase K (PK) were marked.

Figure 3. Continued

(D) Overexpression of WT and cytosolic localized forms of mtSSB, PolG2 and mtDNA-helicase reversed their RNAi rescue effects of *dMterf4RNAi*-mediated defective wing postures.

(E) Overexpression of the cytosolic localized forms of mtSSB, PolG2 and mtDNA-helicase aggravated, while overexpression of their cytosolic localized replication-dead mutants reduced the abnormal wing posture in *dMterf4* knockdown flies.

(F) Knockdown of *dMterf4* decreased the total mtDNA level.

(G) Knockdown of *dMterf4* increased the cytosolic mtDNA level, while simultaneous knockdown of *Med8*, *Tfb4*, *mtSSB*, *PolG2* and *mtDNA-helicase* blocked the upregulation of cytosolic mtDNA levels.

(H) Overexpression of WT and the cytosolic localized forms of mtSSB, PolG2 and mtDNA-helicase increased, while overexpression of cytosolic localized replication-dead mutants decreased the cytosolic mtDNA levels.

(I) Incubating the mitochondria-depleted samples at 25°C for 2 h, the cytosolic mtDNA level was dramatically increased in *dMterf4* knockdown sample. Of note, all cytosolic mtDNA level experiments were performed by removing mitochondria from the cellular extracts.

(J) The Mus mtDNA levels significantly increased in the fly cytosolic extract of *dMterf4* RNAi after 2 h incubation at 25°C. Of note, the cytosolic Mus mtDNA was isolated from the mitochondria-depleted cytosolic extract of C2C12 cells (treated with Rotenone), and then was added into the mitochondria-depleted *Drosophila* cytosolic extracts, with or without incubation at 25°C for 2h, the Mus mtDNA levels were checked.

(K) Overexpression of the cytosolic localized replication-dead mutants of mtSSB, PolG2 and mtDNA-helicase suppressed the increase of Mus mtDNA levels in the fly cytosolic extract of *dMterf4* RNAi after 2 h incubation at 25°C.

(L) The primers of Mus *ND1* gene were specific for detecting Mus cytosolic mtDNA levels. Data are represented as mean ± SD, asterisks indicate statistically significant difference.

them, mtSSBΔ1-47-3xHA could not enter mitochondria due to the lack of an N-terminal mitochondrial localization signal (1–47 aa); Tom20(1–50)-PolG2Δ1-20-3xHA and Tom20(1–50)-mtDNA-helicaseΔ1-33-3xHA anchored on the OMM instead of entering the mitochondrial matrix due to their N-terminal mitochondrial localization signals being replaced by Tom20 transmembrane (TM) sequences (1–50 aa)[39] (Figure S5). Surprisingly, these cytosolic localized forms behaved like their WT to mediate similar abnormal wing phenotypes in their cognate RNAi plus *dMterf4* RNAi background (Figure 3D), indicating that cytosolic localized mtSSB, PolG2 and mtDNA-helicase are sufficient to mediate adverse effects in the *dMterf4* RNAi background.

To further test whether cytosolic localized mtSSB, PolG2 and mtDNA-helicase mediating adverse effects are dependent on their mtDNA replication function, we made replication-dead mutants, including mtSSBΔ1–47/85-91-3xHA, Tom20(1–50)-PolG2Δ1-20-G31E-3xHA and Tom20(1–50)-mtDNA-helicaseΔ1-33-A442P-3xHA. Among them, mtSSBΔ1–47/85-91-3xHA lacked the DNA binding domain (WHRVVVF) situated in 85–91 aa, leading to dramatically reduced mtDNA binding[40]; Tom20(1–50)-PolG2Δ1-20-G31E-3xHA and Tom20(1–50)-mtDNA-helicaseΔ1-33-A442P-3xHA included corresponding mutations, resulting in loss of their enzyme activities.[41,42] Extremely surprisingly, in contrast to their cytosolic localized WT forms, all these cytosolic localized replication-dead mutants, possibly due to their dominant negative function, dramatically reduced the abnormal wing phenotypes in the *dMterf4* RNAi background (Figure 3E), suggesting that cytosolic retained mtSSB, PolG2 and mtDNA-helicase depend on their mtDNA extramitochondrial replication function to mediate *dMterf4* RNAi-triggered adverse effects.

Next, we tested whether cytosolic localized mtSSB, PolG2 and mtDNA-helicase regulate mtDNA cytosolic accumulation in the *dMterf4* RNAi background. Of note, in our study, the cytosolic mtDNA levels were measured by mitochondrial DNA copy numbers, and all cytosolic mtDNA level experiments were performed by removing mitochondria from the cellular extracts. We found that knockdown of *dMterf4* decreased the total mtDNA level of cells but dramatically upregulated the cytosolic mtDNA level through *Med8*, *Tfb4*, *mtSSB*, *PolG2* and *mtDNA-helicase* (Figures 3F and 3G). Consistently, overexpression of cytosolic localized forms of mtSSB, PolG2 and mtDNA-helicase behaved like their WT to dramatically increase the cytosolic mtDNA levels, while overexpression of their cytosolic localized replication-dead mutants decreased the cytosolic mtDNA levels (Figure 3H). Overall, these results suggest that cytosolic localized mtSSB/PolG2/mtDNA-helicase depend on their extramitochondrial mtDNA replication function to dramatically increase the cytosolic mtDNA level of *dMterf4* RNAi flies.

To further test whether extramitochondrial mtDNA replication exists in *dMterf4* RNAi flies, we first made mitochondria-depleted cytosolic extract from *dMterf4* RNAi flies and then incubated this mitochondria-depleted sample at 25°C for 2 h to detect the cytosolic mtDNA level. If extramitochondrial mtDNA replication exists, after incubation, the cytosolic mtDNA level should be increased. Very strikingly, this was the case. After 2 h of incubation, the cytosolic mtDNA level of this mitochondria-depleted cytosolic extract of *dMterf4* RNAi was dramatically increased (Figure 3I), indicating that in this mitochondria-depleted fraction *in vitro* system, cytosolic mtDNA still undergoes replication. Next, to obtain more clean results, we isolated pure mammalian cytosolic mtDNA from mitochondria-depleted cytosolic extract of mouse C2C12 cells and then added it to fly cytosolic mitochondria-depleted extract of *dMterf4* RNAi to verify mammalian mtDNA replication in the fly system. After 2 h of incubation, we found that the C2C12 mtDNA level was also dramatically increased (Figure 3J). Moreover, beginning with the same level of C2C12 mtDNA, compared to the cytosolic localized WT forms, overexpression of the cytosolic localized replication-dead mutants of mtSSB, PolG2 and mtDNA-helicase could suppress the increase in the C2C12 mtDNA level in the fly cytosolic extract of *dMterf4* RNAi after 2 h incubation (Figure 3K). Of note, to avoid possible contamination from fly samples, the selected primers for detecting C2C12 mtDNA levels can only be used to specifically amplify mammalian target genes but not cognate fly homolog genes (Figure 3L). Overall, these results indicate that this *in vitro* cytosolic mitochondria-depleted system of *dMterf4* RNAi includes all needed factors for both fly and mammalian cytosolic mtDNA replication, supporting that cytosolic mtDNA accumulation in *dMterf4* RNAi flies is mainly due to mtDNA extramitochondrial replication mediated by cytosolic retained mtSSB, PolG2 and mtDNA-helicase.
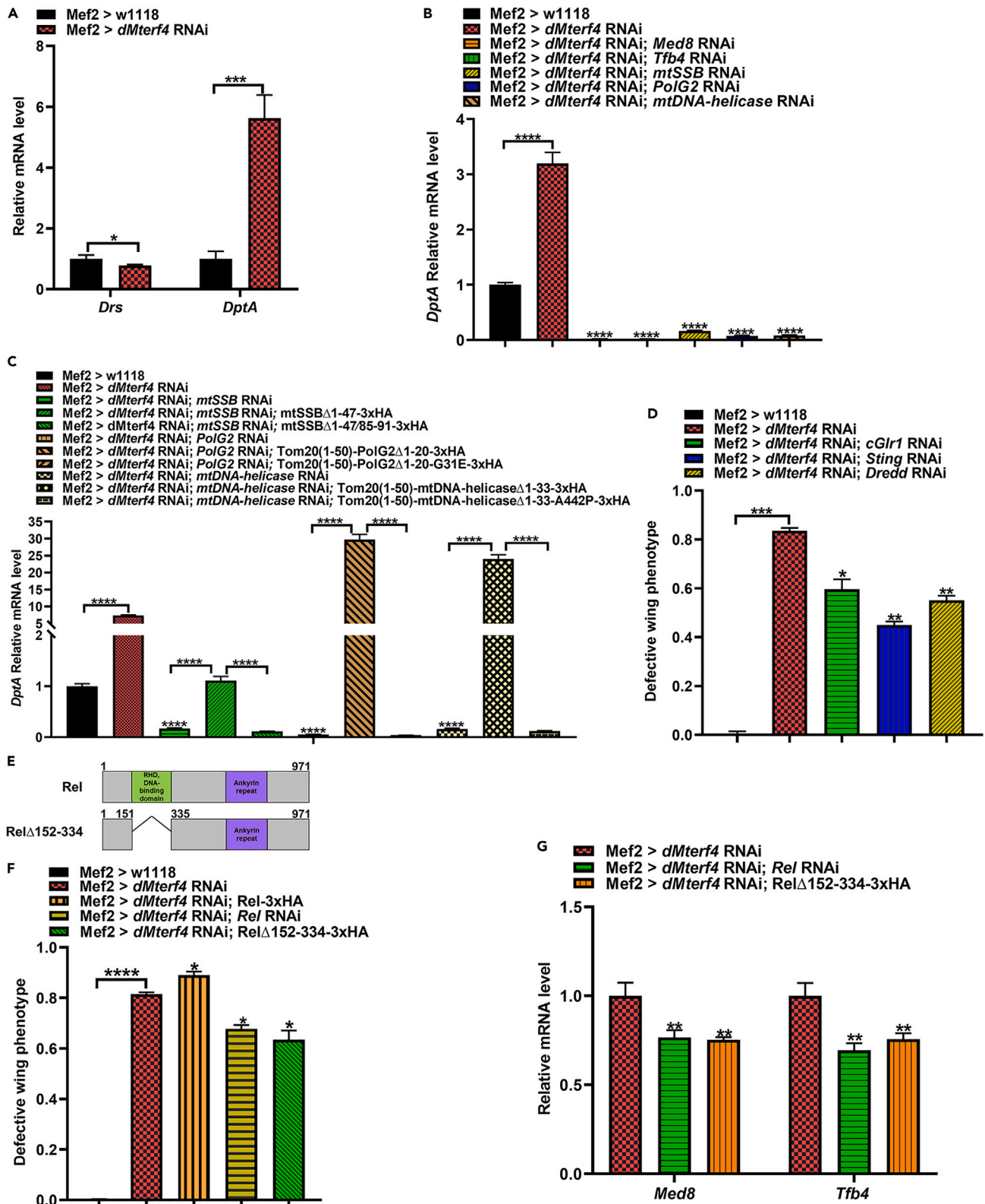
Figure 4. Med8/Tfb4-mtSSB/PolG2/mtDNA-helicase axis-driven cytosolic mtDNA accumulation activates the innate immune response, which partially mediates *dMterf4* RNAi-triggered adverse effects

(A) Knockdown of *dMterf4* upregulated *DptA* mRNA level.

(B) Knockdown of *Med8*, *Tfb4*, *mtSSB*, *PolG2* and *mtDNA-helicase* blocked the upregulated *DptA* mRNA levels in *dMterf4* knockdown flies.

(C) Overexpression of cytosolic localized mtSSBΔ1–47, Tom20(1–50)-PolG2Δ1–20 and Tom20(1–50)-mtDNA-helicaseΔ1–33 activated, while overexpression of their cytosolic localized replication-dead mutants inhibited *DptA* expression.

(D) Knockdown of *cGlr1*, *Sting* and *Dredd* partially rescued the abnormal wing postures in *dMterf4* knockdown flies.

(E) Schematic drawings show Rel and RelΔ152–334.

(F) Knockdown of *Rel* and overexpression of RelΔ152–334 partially rescued the abnormal wing postures in *dMterf4* knockdown flies.

(G) Knockdown of *Rel* and overexpression of RelΔ152-334 decreased *Med8* and *Tfb4* mRNA levels in *dMterf4* knockdown flies. Data are represented as mean ± SD, asterisks indicate statistically significant difference.

Med8/Tfb4-mtSSB/PolG2/mtDNA-helicase axis-driven cytosolic mtDNA accumulation activates the innate immune response, which partially mediates *dMterf4* RNAi-triggered adverse effects

Cytosolic mtDNA can activate innate immune responses,[43,44] so we next detected whether *dMterf4* RNAi-mediated cytosolic mtDNA accumulation can activate fly innate immune responses mediated by the Toll or IMD pathway. By testing the expression of the Toll and IMD pathway target genes *Drs* and *DptA*, we found that knockdown of *dMterf4* dramatically increased *DptA* but not *Drs* transcription through the Med8/Tfb4-mtSSB/PolG2/mtDNA-helicase axis, indicating that its knockdown activates the IMD but not the Toll pathway (Figures 4A and 4B). Next, we further showed that overexpression of cytosolic localized forms of mtSSB/PolG2/mtDNA-helicase increased, while overexpression of their replication-dead mutants decreased, *DptA* transcription in their cognate RNAi background (Figure 4C), indicating that activation of the IMD pathway is dependent on cytosolic mtDNA accumulation mediated by cytosolic mtSSB/PolG2/mtDNA-helicase-triggered mtDNA replication.

As reported, upon cGAS-Sting-like axis activation, the IMD pathway transcription factor Relish (Rel) is cleaved by Dredd to generate the active N-terminus, including the RHD DNA binding domain, which enters the nucleus to induce target gene expression.[45] To further detect whether the IMD pathway is involved in the *dMterf4* RNAi-mediated adverse effects, we knocked down *cGlr1* (the fly cGAS-like receptor 1 gene), *Sting* and *Dredd* in *dMterf4* RNAi flies and found that their knockdown partially rescued the abnormal wing postures of *dMterf4* RNAi flies (Figure 4D). Additionally, we constructed RelΔ152-334-3xHA, which lacked RHD DNA binding domain (Figure 4E), and found that overexpression of Rel aggravated, while overexpression of RelΔ152–334, similar to knockdown of *Rel*, partially rescued *dMterf4* RNAi-mediated abnormal wing postures (Figure 4F). Overall, these results suggest that knockdown of *dMterf4* increases cytosolic mtDNA accumulation, leading to *dMterf4* RNAi-initiated adverse effects, at least, partially through activating the innate immune cGAS-Sting-like signal of the IMD pathway.

Interestingly, we also found that Rel modulated *Med8* and *Tbf4* mRNA levels (Figure 4G), leading to formation of a positive feedback loop to regulate the Med8/Tfb4-mtSSB/PolG2/mtDNA-helicase-Rel axis, suggesting that *dMterf4* RNAi-mediated adverse effects may be partially initiated and amplified by the cGAS-Sting-like signal of the IMD pathway.

The Med8/Tfb4-mtSSB/PolG2/mtDNA-helicase axis affects *Drosophila* lifespan

Given that aging is usually accompanied by mitochondrial decline,[46] we think that it may trigger the Med8/Tfb4-mtSSB/PolG2/mtDNA-helicase axis, leading to accelerated aging and ultimately affecting lifespan. To test this hypothesis, we first detected whether the expression of *Med8* and *Tfb4* is increased upon aging. We selected 3-, 10-, 30- and 50-day-old flies to detect their expression and found that their mRNA levels in indirect flight muscles increased with aging (Figures 5A and 5B). Furthermore, knockdown of *Med8* and *Tfb4* in muscles or dopaminergic neurons with Mef2-Gal4 or TH-Gal4 remarkably extended the lifespan, respectively, while simultaneous overexpression of Med8/MED8 or Tfb4/GTF2H3 reversed and even shortened the lifespan (Figures 5C, 5D, and S6). Overall, these results confirm that the functions of *Med8* and *Tfb4* are conserved and that their knockdown can extend *Drosophila* lifespan. Consistently, knockdown of any mtSSB/PolG2/mtDNA-helicase also extended lifespan (Figure 5E). In addition, taking *mtDNA-helicase* as an example, we found that knockdown of *mtDNA-helicase* could reverse the shortened lifespan caused by overexpression of Fg-Med8/Fg-Tfb4 to levels similar to those of *Med8/Tfb4* RNAi (Figures 5F and 5G), indicating that Med8/Tfb4 regulates *Drosophila* lifespan through mtDNA-helicase. Next, we tested whether the Med8/Tfb4-mtSSB/PolG2/mtDNA-helicase axis modulates lifespan by regulating cytosolic mtDNA accumulation. We found that the cytosolic mtDNA in indirect flight muscles was increased during aging. The level in 50-day-old flies was significantly higher than that in 3-day-old flies (Figure 5H), and knockdown of *Med8* and *Tfb4* dramatically reduced cytosolic mtDNA levels in 50-day-old flies (Figure 5I). To further investigate whether the increased cytosolic mtDNA could regulate lifespan, we overexpressed the WT, cytosolic localized forms of mtSSB/PolG2/mtDNA-helicase to increase the cytosolic mtDNA levels (Figure 5J) and found that their overexpression dramatically reduced lifespan (Figure 5K). In contrast, when overexpressing cytosolic localized replication-dead mutants of mtSSB/PolG2/mtDNA-helicase to reduce the cytosolic mtDNA level (Figure 5L), we found that their overexpression extended lifespan (Figure 5M). Overall, these results suggest that during aging, increased mitochondrial defects may cause cytosolic mtDNA accumulation through the Med8/Tfb4-mtSSB/PolG2/mtDNA-helicase axis, leading to accelerated aging, implying that the increased cytosolic mtDNA is one of the major triggers of aging.
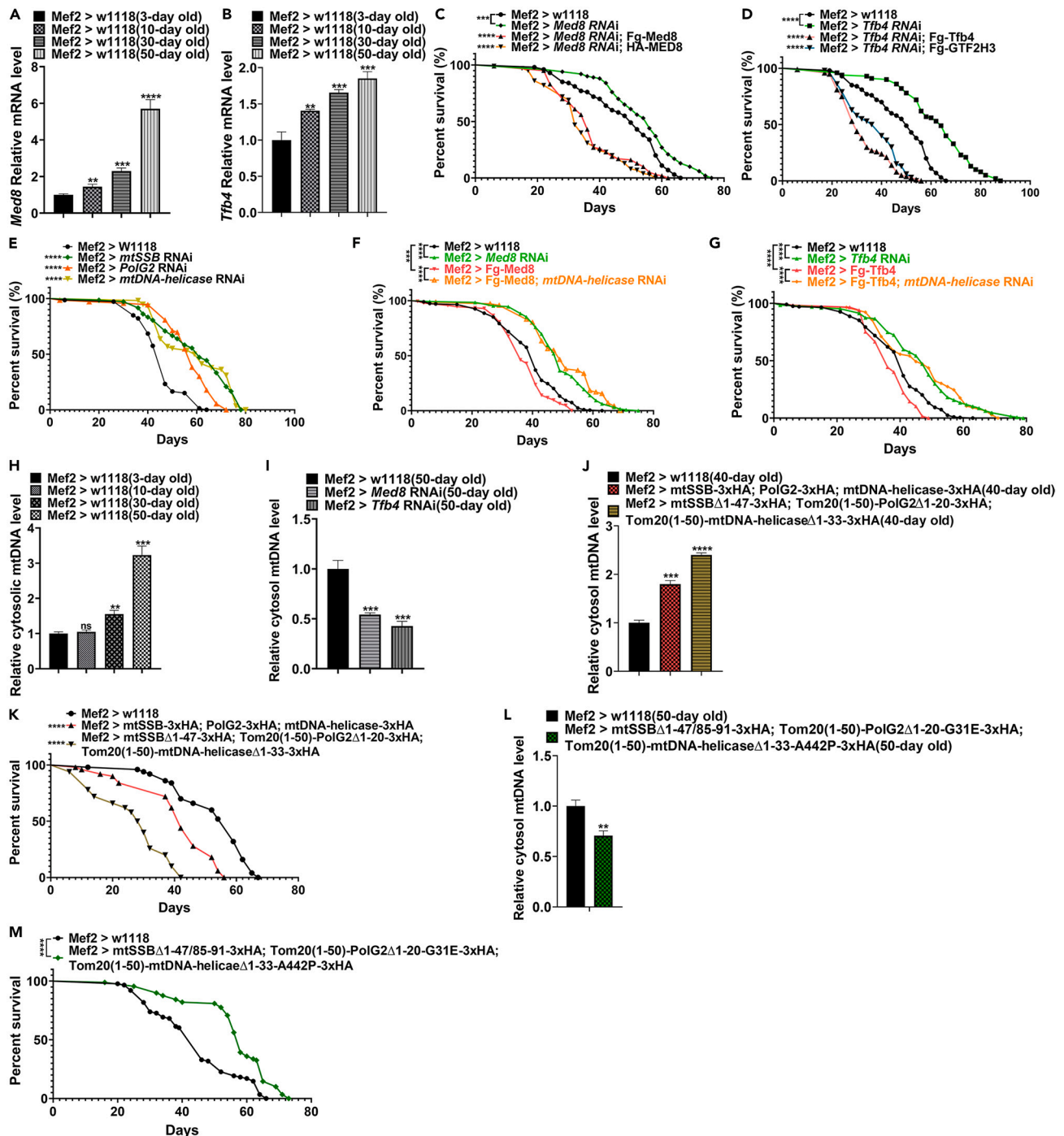
Figure 5. The Med8/Tfb4-mtSSB/PolG2/mtDNA-helicase axis affects *Drosophila* lifespan

(A and B) The mRNA levels of *Med8* and *Tfb4* increased with aging.

(C and D) Compared with control, knockdown of *Med8* and *Tfb4* remarkably extended fly lifespan. While cooverexpression of Med8/MED8 and Tfb4/GTF2H3 reversed *Med8* and *Tfb4* RNAis-mediated extended lifespan, respectively.

(E) Knockdown of *mtSSB*, *PolG2* and *mtDNA-helicase* extended lifespan.

(F and G) Knockdown of *mtDNA-helicase* reversed shortened lifespan caused by overexpression of Fg-Med8/Fg-Tfb4 to similar levels of those of *Med8*/*Tfb4* RNAis, respectively.

(H) The cytosolic mtDNA levels increased with aging.

(I) Knockdown of *Med8* and *Tfb4* decreased the cytosolic mtDNA levels in 50-day-old flies.

Figure 5. Continued

(J) Cooverexpression of WT or cytosolic localized mtSSB/PolG2/mtDNA-helicase significantly increased the cytosolic mtDNA levels in 40-day-old flies.

(K) Cooverexpression of mtSSB/PolG2/mtDNA-helicase dramatically reduced lifespan.

(L) Cooverexpression of the cytosolic localized replication-dead mutants of mtSSB, PolG2 and mtDNA-helicase decreased the cytosolic mtDNA level in old flies.

(M) Cooverexpression of the cytosolic localized replication-dead mutants of mtSSB, PolG2 and mtDNA-helicase extended lifespan. Data are represented as mean ± SD, asterisks indicate statistically significant difference.

DISCUSSION

Compromised mitochondrial function is a crucial factor contributing to multiple human diseases; however, the *in vivo* rescue signal of such mitochondrial defect effects is not clear. In this study, we identified that Med8, Tfb4, mtSSB, PolG2 and mtDNA-helicase mediated the *dMterf4* RNAi-triggered adverse effects through the Med8/Tfb4-mtSSB/PolG2/mtDNA-helicase axis. Extremely surprisingly, we found that extramitochondrial mtDNA could replicate and that this Med8/Tfb4-mtSSB/PolG2/mtDNA-helicase axis-driven cytosolic mtDNA replication mediated mitochondrial defect-initiated adverse effects. Importantly, we found that this regulatory mechanism was also applied for many other fly mitochondrial gene-related mitochondrial dysfunctions, suggesting that the Med8/Tfb4-mtSSB/PolG2/mtDNA-helicase axis may function as a broader common signal to modulate mitochondrial defect effects. In addition, we found that the above regulatory mechanism was also involved in fly aging, indicating that Med8/Tfb4-mtSSB/PolG2/mtDNA-helicase axis-driven cytosolic mtDNA accumulation plays an important role in aging. Except for flies, in mammalian C2C12 cells, the change in mammalian cytosolic mtDNA levels after 2 h of incubation also implied mtDNA extramitochondrial replication (Figure S7). Overall, our results suggest that the Med8/Tfb4-mtSSB/PolG2/mtDNA-helicase axis might serve as a potential therapeutic target for related mitochondrial and age-related diseases. Of note, because *PolrMT* RNAi was missed in our screen library, we did not obtain it in our rescue list. During the revision of this manuscript, we found that *PolrMT* mRNA levels were also increased in *dMterf4* knockdown flies (Figure S8A). Using a reordered *PolrMT* RNAi line, we found that, similar to knockdown of *mtSSB*, *PolG2* and *mtDNA-helicase*, knockdown of *PolrMT* partially rescued the *dMterf4* RNAi-mediated wing phenotype and reduced the cytosolic mtDNA level (Figures S8B and S8C), supporting PolrMT together with mtSSB, PolG2 and mtDNA-helicase mediating *dMterf4* RNAi-triggered adverse effects.

Our results demonstrated that knockdown of *dMterf4* not only upregulated the transcription of *Med8* and *Tfb4* but also promoted Tfb4 translocation into the nucleus, indicating that knockdown of *dMterf4* regulates the transcription of *mtSSB*, *PolG2* and *mtDNA-helicase* in multiple layers. However, how knockdown of *dMterf4* increases the transcription of *Med8* and *Tfb4* and facilitates Tfb4 translocation into the nucleus is not clear. Interestingly, when we further tested whether *mtSSB*, *PolG2* and *mtDNA-helicase* regulate *Med8* and *Tfb4* in a feedback manner, we found that knockdown of them decreased the transcription of *Tfb4*, and Med8 and Tfb4 positively regulated each other in *dMterf4* knockdown flies (Figures S4F and S4G). Similar results were obtained for Rel, which modulated *Med8* and *Tbf4* mRNA levels (Figure 4G), indicating that the Med8/Tfb4-mtSSB/PolG2/mtDNA-helicase-Rel axis forms a positive feedback loop to regulate the cytosolic mtDNA level, leading to efficient amplification of the *dMterf4* RNAi-mediated adverse effects. The results also imply that *dMterf4* RNAi-mediated cytosolic mtDNA release may partially initiate this signaling axis through upregulation of *Med8* and *Tbf4* transcription by the cGAS-Sting-like signal of the IMD pathway.

Med8 as one subunit of the mediator complex may bridge the gene-specific transcription factor and the general transcription factor Tfb4 to regulate *mtSSB*, *PolG2* and *mtDNA-helicase* transcription. What is specific transcription factor of these genes? Previous studies reported that transcription of *mtSSB*, *PolG2* and *mtDNA-helicase* is regulated by Dref,[47] which prompted us to test whether Dref is the specific transcription factor that, together with Med8/Tfb4, regulates *mtSSB*, *PolG2* and *mtDNA-helicase* transcription. We found that Med8 bound with Dref, and knockdown of *Dref* decreased the transcription of *mtSSB*, *PolG2* and *mtDNA-helicase*, and partially rescued the abnormal wing postures of *dMterf4* RNAi flies (Figures S4H–S4J), indicating that Dref indeed functions as a specific transcription factor together with Med8/Tfb4 partially to regulate the transcription of *mtSSB*, *PolG2* and *mtDNA-helicase*. Of note, our results cannot rule out that other specific transcription factors may be involved in the regulation of *mtSSB*, *PolG2* and *mtDNA-helicase* transcription.

In *dMerf4* RNAi flies, cytosolic mtDNA levels were dramatically increased, which mediated *dMerf4* RNAi-related phenotypes. There are some possibilities for the increase of cytosolic mtDNA level: (A) The *dMerf4* RNAi flies experienced elevated levels of mtDNA secretion from the mitochondria; (B) the mitochondrial-derived vesicles (MDVs) contributed to the increase of cytosolic mtDNA level; (C) the cytosolic accumulation of mtDNA was amplified through extramitochondrial mtDNA replication we demonstrated in this study. Cytosolic mtDNA can activate innate immune pathways. In mammals, mtDNA that escapes to the cytosol from damaged mitochondria is recognized by cGAS and signals through cGAMP and Sting to activate inflammatory gene transcription. Vesicle-related cytosolic mtDNAs including those mediated by MDVs tend to bind endosomal TLR9, triggering MyD88-dependent signaling to interferons and proinflammatory cytokines.[48–51] The mammalian cGAS-Sting and TLR9 signaling pathways correspond to *Drosophila* IMD and Toll pathways, respectively. However, in our *dMerf4* RNAi case, cytosolic mtDNA only activated IMD but not the Toll pathway, implying that cytosolic mtDNA activates the fly innate immune response less possibly through MDVs. When further knocking down the MDV mediating factor genes *dSNX9*, *pink1* and *parkin*,[49] we found that their knockdown also did not rescue the *dMerf4* RNAi-mediated death phenotype under 29°C (Figure S9A), supporting that the *dMerf4* RNAi phenotype is not mainly triggered via MDVs. Afterward, we tested where the main cytosolic mtDNA activating the IMD pathway was from in *dMerf4* RNAi flies and found that knocking down mtDNA cytosolic release-related genes including *porin*, *buffy*, *debcl*, *sesB* and *phb1*[52,53] also did not rescue the *dMerf4* RNAi-mediated death phenotype under 29°C (Figure S9B), implying that even though cytosolic release of mtDNA may contribute to the accumulation of cytosolic mtDNA, this is not the primary cause.

Interestingly, we found that knockdown of *dMterf4* upregulated Med8/Tbf4 levels, leading to the upregulation of mtSSB, PolG2 and mtDNA-helicase, which were stuck in the cytosol (Figures 3A–3C) to mainly mediate extramitochondrial mtDNA replication. In this situation, knockdown of these genes could largely rescue *dMterf4* RNAi-triggered adverse effects (Figures 2A–2L and S2), supporting that Med8/Tfb4-mtSSB/PolG2/mtDNA-helicase axis-mediated extramitochondrial mtDNA replication is mainly responsible for cytosolic mtDNA accumulation. This conclusion is also supported by in *dMterf4* knockdown context, overexpression of the cytosolic localized replication-dead mutant of PolG2 suppressing the increase in the cytosolic mtDNA level by more than 50%, regardless of its efficiency (Figure S10). Moreover, *in vivo* extramitochondrial mtDNA replication was manifested by cytosolic localized forms of mtSSB/PolG2/mtDNA-helicase and their replication-dead mutants still dramatically but conversely regulated cytosolic mtDNA levels and wing phenotypes in a replication activity-dependent manner (Figures 3D, 3E, and 3H). More clearly, in Figure 3H, if not regulating extramitochondrial mtDNA replication, cytosolic localized WT and mutation forms of mtSSB, PolG2, mtDNA-helicase which no longer enter mitochondrial matrix should not affect cytosolic mtDNA levels of *dMerf4* RNAi flies in their cognate RNAi background, respectively; but actually they still affected the cytosolic mtDNA levels. In addition, extramitochondrial mtDNA replication was also manifested by *in vitro* both fly and mammalian cytosolic mtDNA levels in their mitochondria-depleted cellular extracts being dramatically increased after just 2 h incubation at 25°C and 37°C, respectively (Figures 3I and S7C). In particular, the isolated mammalian pure cytosolic mtDNA could be amplified in the fly system, and cytosolic localized replication-dead mutants of mtSSB, PolG2 and mtDNA-helicase could suppress the increase in the C2C12 mtDNA level in the fly cytosolic extract of *dMterf4* RNAi after 2 h of incubation (Figures 3J and 3K), implying that these mammalian mtDNA undergoes extramitochondrial replication in the fly system. Of note, the selected primers for detecting mammalian C2C12 mtDNA levels can only be used to specifically amplify mammalian target genes but not cognate fly homolog genes, which rules out the interference of fly mtDNA from fly cytosolic mitochondria-depleted extracts of *dMterf4* RNAi (Figure 3L). Overall, these results suggest that the above mitochondria-depleted fly cellular extract of *dMterf4* RNAi includes all necessary components for both fly and mammalian cytosolic mtDNA replication, which may be largely due to cytosolic retention of mitochondrial mtDNA replication-related proteins, such as mtSSB, PolG2, mtDNA-helicase and PolrMT. The underlying detailed mechanism awaits further study.

We demonstrated that *dMterf4* RNAi triggered mitochondrial defect effects through replication-mediated cytosolic mtDNA accumulation. However, how cytosolic mtDNA accumulation mediates adverse effects is elusive. We found that cytosolic mtDNA could dramatically activate the fly innate immune IMD pathway. When checking whether the activated IMD pathway mediates adverse effects, we found that inhibition of the IMD pathway only partially rescued *dMterf4* RNAi-mediated adverse effects, suggesting that in addition to the IMD pathway, there are other signals that together mediate *dMterf4* RNAi-triggered mitochondrial defects.

It is well known that mitochondrial dysfunction is one of the main causes of cell senescence and biological aging.[46,54] However, how mitochondrial dysfunction is related to aging is elusive. In this study, we strikingly found that cytosolic mtDNA gradually increased during aging, which was controlled by Med8 and Tfb4. Modulating the Med8/Tfb4-mtSSB/PolG2/mtDNA-helicase axis changed cytosolic mtDNA levels, leading to significant effects on fly lifespan, suggesting that cytosolic mtDNA accumulation is one of the major triggers of aging and that suppressing cytosolic mtDNA accumulation may extend lifespan.

In summary, multiple mitochondrial defects may promote cytosolic release of mtDNA, increase cytosolic retention of mtSSB/PolG2/mtDNA-helicase and upregulate Med8/Tfb4 levels, resulting in amplification of Med8/Tfb4-mtSSB/PolG2/mtDNA-helicase axis signaling. All these factors work together to strongly drive mtDNA extramitochondrial replication, leading to mitochondrial dysfunction-related diseases and aging. Our study indicates that this regulatory axis might serve as a potential therapeutic target for mitochondrial and age-related diseases.

Limitations of the study

We demonstrated that the Med8/Tfb4-mtSSB/PolG2/mtDNA-helicase axis drove mtDNA extramitochondrial replication to expand the cytosolic mtDNA, resulting in the *dMterf4* RNAi-mediated mitochondrial defect effects. However, inhibition of the IMD pathway only partially rescued the adverse effects mediated by *dMterf4* RNAi, suggesting that in addition to the IMD pathway, other signals co-mediate mitochondrial defects triggered by *dMterf4* RNAi. These involved signals require further investigation to fully understand how cytosolic mtDNA accumulation mediates *dMterf4* RNAi-mediated adverse effects. In addition, more experiments are needed to address that the Med8/Tfb4-mtSSB/PolG2/mtDNA-helicase axis mediates mitochondrial defect effects by driving mtDNA extramitochondrial replication in mammalian cells and mammals.

STAR★METHODS

Detailed methods are provided in the online version of this paper and include the following:

- KEY RESOURCES TABLE
- RESOURCE AVAILABILITY
  - ○ Lead contact
  - ○ Materials availability
  - ○ Data and code availability
- EXPERIMENTAL MODEL AND STUDY PARTICIPANT DETAILS
  - ○ *Drosophila* genetics

- ○ Cell culture and transfection
- ● METHOD DETAILS
  - ○ Climbing assay
  - ○ Lifespan analysis
  - ○ ATP assay
  - ○ Immunohistochemistry
  - ○ RNA extraction and quantitative RT-PCR
  - ○ Western blot and immunoprecipitation
  - ○ Relative cytosolic mtDNA copy number measurement
- ● QUANTIFICATION AND STATISTICS ANALYSIS
  - ○ Statistics

SUPPLEMENTAL INFORMATION

Supplemental information can be found online at https://doi.org/10.1016/j.isci.2024.108970.

AUTHOR CONTRIBUTIONS

Q.Z. conceived the project. Z.S., Y.W., and Q.Z. designed the experiments. Z.S., S.L., Y.G., C.J., X.T., H.Z., Y.W., G.Z., and Y.W. performed the experiments. Z.S., S.L., Y.G., Y.W., and Q.Z. conducted the data analysis. S.L., Y.W., and Q.Z. wrote the manuscript. All authors read and edited the manuscript.

DECLARATION OF INTERESTS

The authors declare no competing interests.

REFERENCES

1. Vercellino, I., and Sazanov, L.A. (2022). The assembly, regulation and function of the mitochondrial respiratory chain. Nat. Rev. Mol. Cell Biol. 23, 141–161. https://doi.org/10.1038/s41580-021-00415-0.

2. Pagliarini, D.J., and Rutter, J. (2013). Hallmarks of a new era in mitochondrial biochemistry. Genes Dev. 27, 2615–2627. https://doi.org/10.1101/gad.229724.113.

3. Becker, Y.L.C., Duvvuri, B., Fortin, P.R., Lood, C., and Boilard, E. (2022). The role of mitochondria in rheumatic diseases. Nat. Rev. Rheumatol. 18, 621–640. https://doi.org/10.1038/s41584-022-00834-z.

4. Frey, T.G., and Mannella, C.A. (2000). The internal structure of mitochondria. Trends Biochem. Sci. 25, 319–324. https://doi.org/10.1016/s0968-0004(00)01609-1.

5. Rackham, O., and Filipovska, A. (2022). Organization and expression of the mammalian mitochondrial genome. Nat. Rev. Genet. 23, 606–623. https://doi.org/10.1038/s41576-022-00480-x.

6. Yan, C., Duanmu, X., Zeng, L., Liu, B., and Song, Z. (2019). Mitochondrial DNA: Distribution, Mutations, and Elimination. Cells 8. https://doi.org/10.3390/cells8040379.

7. Quiles, J.M., and Gustafsson, Å.B. (2022). The role of mitochondrial fission in cardiovascular health and disease. Nat. Rev. Cardiol. 19, 723–736. https://doi.org/10.1038/s41569-022-00703-y.

8. Chan, D.C. (2006). Mitochondria: dynamic organelles in disease, aging, and development. Cell 125, 1241–1252. https://doi.org/10.1016/j.cell.2006.06.010.

9. Anderson, S., Bankier, A.T., Barrell, B.G., de Bruijn, M.H., Coulson, A.R., Drouin, J., Eperon, I.C., Nierlich, D.P., Roe, B.A., Sanger, F., et al. (1981). Sequence and organization of the human mitochondrial genome. Nature 290, 457–465. https://doi.org/10.1038/290457a0.

10. Lee, C., Kim, K.H., and Cohen, P. (2016). MOTS-c: A novel mitochondrial-derived peptide regulating muscle and fat metabolism. Free Radic. Biol. Med. 100, 182–187. https://doi.org/10.1016/j.freeradbiomed.2016.05.015.

11. Ryan, M.T., and Hoogenraad, N.J. (2007). Mitochondrial-nuclear communications. Annu. Rev. Biochem. 76, 701–722. https://doi.org/10.1146/annurev.biochem.76.052305.091720.

12. Friedman, J.R., and Nunnari, J. (2014). Mitochondrial form and function. Nature 505, 335–343. https://doi.org/10.1038/nature12985.

13. Almannai, M., El-Hattab, A.W., and Scaglia, F. (2018). Mitochondrial DNA replication: clinical syndromes. Essays Biochem. 62, 297–308. https://doi.org/10.1042/EBC20170101.

14. Jiang, M., Xie, X., Zhu, X., Jiang, S., Milenkovic, D., Misic, J., Shi, Y., Tandukar, N., Li, X., Atanassov, I., et al. (2021). The mitochondrial single-stranded DNA binding protein is essential for initiation of mtDNA replication. Sci. Adv. 7, eabf8631. https://doi.org/10.1126/sciadv.abf8631.

15. Kaguni, L.S. (2004). DNA polymerase gamma, the mitochondrial replicase. Annu. Rev. Biochem. 73, 293–320. https://doi.org/10.1146/annurev.biochem.72.121801.161455.

16. Sen, D., Patel, G., and Patel, S.S. (2016). Homologous DNA strand exchange activity of the human mitochondrial DNA helicase TWINKLE. Nucleic Acids Res. *44*, 4200–4210. https://doi.org/10.1093/nar/gkw098.

17. Korhonen, J.A., Pham, X.H., Pellegrini, M., and Falkenberg, M. (2004). Reconstitution of a minimal mtDNA replisome in vitro. EMBO J. *23*, 2423–2429. https://doi.org/10.1038/sj.emboj.7600257.

18. Fontana, G.A., and Gahlon, H.L. (2020). Mechanisms of replication and repair in mitochondrial DNA deletion formation. Nucleic Acids Res. *48*, 11244–11258. https://doi.org/10.1093/nar/gkaa804.

19. Falkenberg, M. (2018). Mitochondrial DNA replication in mammalian cells: overview of the pathway. Essays Biochem. *62*, 287–296. https://doi.org/10.1042/EBC20170100.

20. He, W.R., Cao, L.B., Yang, Y.L., Hua, D., Hu, M.M., and Shu, H.B. (2021). VRK2 is involved in the innate antiviral response by promoting mitostress-induced mtDNA release. Cell. Mol. Immunol. *18*, 1186–1196. https://doi.org/10.1038/s41423-021-00673-0.

21. McArthur, K., Whitehead, L.W., Heddleston, J.M., Li, L., Padman, B.S., Oorschot, V., Geoghegan, N.D., Chappaz, S., Davidson, S., San Chin, H., et al. (2018). BAK/BAX macropores facilitate mitochondrial herniation and mtDNA efflux during apoptosis. Science *359*, eaao6047. https://doi.org/10.1126/science.aao6047.

22. Cosentino, K., Hertlein, V., Jenner, A., Dellmann, T., Gojkovic, M., Peña-Blanco, A., Dadsena, S., Wajngarten, N., Danial, J.S.H., Thevathasan, J.V., et al. (2022). The interplay between BAX and BAK tunes apoptotic pore growth to control mitochondrial-DNA-mediated inflammation. Mol. Cell *82*, 933–949.e9. https://doi.org/10.1016/j.molcel.2022.01.008.

23. Kim, J., Gupta, R., Blanco, L.P., Yang, S., Shteinfer-Kuzmine, A., Wang, K., Zhu, J., Yoon, H.E., Wang, X., Kerkhofs, M., et al. (2019). VDAC oligomers form mitochondrial pores to release mtDNA fragments and promote lupus-like disease. Science *366*, 1531–1536. https://doi.org/10.1126/science.aav4011.

24. Yan, J., Liu, W., Feng, F., and Chen, L. (2020). VDAC oligomer pores: A mechanism in disease triggered by mtDNA release. Cell Biol. Int. *44*, 2178–2181. https://doi.org/10.1002/cbin.11427.

25. Yu, C.H., Davidson, S., Harapas, C.R., Hilton, J.B., Mlodzianoski, M.J., Laohamonthonkul, P., Louis, C., Low, R.R.J., Moecking, J., De Nardo, D., et al. (2020). TDP-43 Triggers Mitochondrial DNA Release via mPTP to Activate cGAS/STING in ALS. Cell *183*, 636–649.e18. https://doi.org/10.1016/j.cell.2020.09.020.

26. Riley, J.S., and Tait, S.W. (2020). Mitochondrial DNA in inflammation and immunity. EMBO Rep. *21*, e49799. https://doi.org/10.15252/embr.201949799.

27. De Gaetano, A., Solodka, K., Zanini, G., Selleri, V., Mattioli, A.V., Nasi, M., and Pinti, M. (2021). Molecular Mechanisms of mtDNA-Mediated Inflammation. Cells *10*, 2898. https://doi.org/10.3390/cells10112898.

28. Chowdhury, A., Witte, S., and Aich, A. (2022). Role of Mitochondrial Nucleic Acid Sensing Pathways in Health and Patho-Physiology. Front. Cell Dev. Biol. *10*, 796066. https://doi.org/10.3389/fcell.2022.796066.

29. Ablasser, A., and Chen, Z.J. (2019). cGAS in action: Expanding roles in immunity and inflammation. Science *363*, eaat8657. https://doi.org/10.1126/science.aat8657.

30. Sladowska, M., Turek, M., Kim, M.J., Drabikowski, K., Mussulini, B.H.M., Mohanraj, K., Serwa, R.A., Topf, U., and Chacinska, A. (2021). Proteasome activity contributes to pro-survival response upon mild mitochondrial stress in Caenorhabditis elegans. PLoS Biol. *19*, e3001302. https://doi.org/10.1371/journal.pbio.3001302.

31. Diao, R.Y., and Gustafsson, Å.B. (2022). Mitochondrial quality surveillance: mitophagy in cardiovascular health and disease. Am. J. Physiol. Cell Physiol. *322*, C218–C230. https://doi.org/10.1152/ajpcell.00360.2021.

32. Mottis, A., Herzig, S., and Auwerx, J. (2019). Mitocellular communication: Shaping health and disease. Science *366*, 827–832. https://doi.org/10.1126/science.aax3768.

33. Nunnari, J., and Suomalainen, A. (2012). Mitochondria: in sickness and in health. Cell *148*, 1145–1159. https://doi.org/10.1016/j.cell.2012.02.035.

34. Lu, B., and Vogel, H. (2009). Drosophila models of neurodegenerative diseases. Annu. Rev. Pathol. *4*, 315–342. https://doi.org/10.1146/annurev.pathol.3.121806.151529.

35. Cámara, Y., Asin-Cayuela, J., Park, C.B., Metodiev, M.D., Shi, Y., Ruzzenente, B., Kukat, C., Habermann, B., Wibom, R., Hultenby, K., et al. (2011). MTERF4 regulates translation by targeting the methyltransferase NSUN4 to the mammalian mitochondrial ribosome. Cell Metabol. *13*, 527–539. https://doi.org/10.1016/j.cmet.2011.04.002.

36. Kohda, M., Tokuzawa, Y., Kishita, Y., Nyuzuki, H., Moriyama, Y., Mizuno, Y., Hirata, T., Yatsuka, Y., Yamashita-Sugahara, Y., Nakachi, Y., et al. (2016). A Comprehensive Genomic Analysis Reveals the Genetic Landscape of Mitochondrial Respiratory Chain Complex Deficiencies. PLoS Genet. *12*, e1005679. https://doi.org/10.1371/journal.pgen.1005679.

37. Boube, M., Joulia, L., Cribbs, D.L., and Bourbon, H.M. (2002). Evidence for a mediator of RNA polymerase II transcriptional regulation conserved from yeast to man. Cell *110*, 143–151. https://doi.org/10.1016/s0092-8674(02)00830-9.

38. Gutiérrez, L., Merino, C., Vázquez, M., Reynaud, E., and Zurita, M. (2004). RNA polymerase II 140wimp mutant and mutations in the TFIIH subunit XPB differentially affect homeotic gene expression in Drosophila. Genesis *40*, 58–66. https://doi.org/10.1002/gene.20066.

39. Abe, Y., Shodai, T., Muto, T., Mihara, K., Torii, H., Nishikawa, S., Endo, T., and Kohda, D. (2000). Structural basis of presequence recognition by the mitochondrial protein import receptor Tom20. Cell *100*, 551–560. https://doi.org/10.1016/s0092-8674(00)80691-1.

40. Farr, C.L., Matsushima, Y., Lagina, A.T., 3rd, Luo, N., and Kaguni, L.S. (2004). Physiological and biochemical defects in functional interactions of mitochondrial DNA polymerase and DNA-binding mutants of single-stranded DNA-binding protein. J. Biol. Chem. *279*, 17047–17053. https://doi.org/10.1074/jbc.M400283200.

41. Iyengar, B., Luo, N., Farr, C.L., Kaguni, L.S., and Campos, A.R. (2002). The accessory subunit of DNA polymerase gamma is essential for mitochondrial DNA maintenance and development in Drosophila melanogaster. Proc. Natl. Acad. Sci. USA *99*, 4483–4488. https://doi.org/10.1073/pnas.072664899.

42. Sanchez-Martinez, A., Calleja, M., Peralta, S., Matsushima, Y., Hernandez-Sierra, R., Whitworth, A.J., Kaguni, L.S., and Garesse, R. (2012). Modeling pathogenic mutations of human twinkle in Drosophila suggests an apoptosis role in response to mitochondrial defects. PLoS One *7*, e43954. https://doi.org/10.1371/journal.pone.0043954.

43. Banoth, B., and Cassel, S.L. (2018). Mitochondria in innate immune signaling. Transl. Res. *202*, 52–68. https://doi.org/10.1016/j.trsl.2018.07.014.

44. West, A.P., and Shadel, G.S. (2017). Mitochondrial DNA in innate immune responses and inflammatory pathology. Nat. Rev. Immunol. *17*, 363–375. https://doi.org/10.1038/nri.2017.21.

45. Ganesan, S., Aggarwal, K., Paquette, N., and Silverman, N. (2011). NF-kappaB/Rel proteins and the humoral immune responses of Drosophila melanogaster. Curr. Top. Microbiol. Immunol. *349*, 25–60. https://doi.org/10.1007/82_2010_107.

46. Miwa, S., Kashyap, S., Chini, E., and von Zglinicki, T. (2022). Mitochondrial dysfunction in cell senescence and aging. J. Clin. Invest. *132*, e158447. https://doi.org/10.1172/JCI158447.

47. Tue, N.T., Yoshioka, Y., Mizoguchi, M., Yoshida, H., Zurita, M., and Yamaguchi, M. (2017). DREF plays multiple roles during Drosophila development. Biochim. Biophys. Acta. Gene Regul. Mech. *1860*, 705–712. https://doi.org/10.1016/j.bbagrm.2017.03.004.

48. Hazan Ben-Menachem, R., Lintzer, D., Ziv, T., Das, K., Rosenhek-Goldian, I., Porat, Z., Ben Ami Pilo, H., Karniely, S., Saada, A., Regev-Rudzki, N., and Pines, O. (2023). Mitochondrial-derived vesicles retain membrane potential and contain a functional ATP synthase. EMBO Rep. *24*, e56114. https://doi.org/10.15252/embr.202256114.

49. Sugiura, A., McLelland, G.L., Fon, E.A., and McBride, H.M. (2014). A new pathway for mitochondrial quality control: mitochondrial-derived vesicles. EMBO J. *33*, 2142–2156. https://doi.org/10.15252/embj.201488104.

50. Zecchini, V., Paupe, V., Herranz-Montoya, I., Janssen, J., Wortel, I.M.N., Morris, J.L., Ferguson, A., Chowdury, S.R., Segarra-Mondejar, M., Costa, A.S.H., et al. (2023). Fumarate induces vesicular release of mtDNA to drive innate immunity. Nature *615*, 499–506. https://doi.org/10.1038/s41586-023-05770-w.

51. Andrade-Navarro, M.A., Sanchez-Pulido, L., and McBride, H.M. (2009). Mitochondrial vesicles: an ancient process providing new links to peroxisomes. Curr. Opin. Cell Biol. *21*, 560–567. https://doi.org/10.1016/j.ceb.2009.04.005.

52. Liu, H., Fan, H., He, P., Zhuang, H., Liu, X., Chen, M., Zhong, W., Zhang, Y., Zhen, C., Li, Y., et al. (2022). Prohibitin 1 regulates mtDNA release and downstream inflammatory responses. EMBO J. *41*, e111173. https://doi.org/10.15252/embj.2022111173.

53. Harris, M.H., and Thompson, C.B. (2000). The role of the Bcl-2 family in the regulation of outer mitochondrial membrane permeability. Cell Death Differ. *7*, 1182–1191. https://doi.org/10.1038/sj.cdd.4400781.

54. Jang, J.Y., Blum, A., Liu, J., and Finkel, T. (2018). The role of mitochondria in aging. J. Clin. Invest. *128*, 3662–3670. https://doi.org/10.1172/JCI120842.

55. Liu, W., Duan, X., Xu, L., Shang, W., Zhao, J., Wang, L., Li, J.C., Chen, C.H., Liu, J.P., and Tong, C. (2020). Chchd2 regulates mitochondrial morphology by modulating the levels of Opa1. Cell Death Differ. *27*, 2014–2029. https://doi.org/10.1038/s41418-019-0482-7.

56. Mohammadian Gol, T., Rodemann, H.P., and Dittmann, K. (2019). Depletion of Akt1 and Akt2 Impairs the Repair of Radiation-Induced DNA Double Strand Breaks via Homologous Recombination. Int. J. Mol. Sci. *20*, 6316. https://doi.org/10.3390/ijms20246316.

57. Xu, Z., Fu, T., Guo, Q., Zhou, D., Sun, W., Zhou, Z., Chen, X., Zhang, J., Liu, L., Xiao, L., et al. (2022). Disuse-associated loss of the protease LONP1 in muscle impairs mitochondrial function and causes reduced skeletal muscle mass and strength. Nat. Commun. *13*, 894. https://doi.org/10.1038/s41467-022-28557-5.

58. Salminen, T.S., Oliveira, M.T., Cannino, G., Lillsunde, P., Jacobs, H.T., and Kaguni, L.S. (2017). Mitochondrial genotype modulates mtDNA copy number and organismal phenotype in Drosophila. Mitochondrion *34*, 75–83. https://doi.org/10.1016/j.mito.2017.02.001.

STAR★METHODS

KEY RESOURCES TABLE

REAGENT or RESOURCE	SOURCE	IDENTIFIER
Antibodies		
Mouse monoclonal anti-ATP5A	Abcam	Cat#15H4C4; RRID: AB_301447
Mouse monoclonal anti-HA	Santa Cruz	Cat# sc-7392; RRID: AB_627809
Mouse monoclonal anti-Tubulin	DHSB	Cat#6G7; RRID: AB_528497
Mouse monoclonal anti-Flag	Sigma	Cat#F4049; RRID: AB_439701
Mouse monoclonal anti-Actin	Genscript	Cat#A00702; RRID: AB_914102
Goat anti-mouse Ig-G antibody	Jackson ImmunoResearch	Cat#115-545-003; RRID: AB_2338840
Donkey anti-mouse IgG conjugated to Cy3	Jackson ImmunoResearch	Cat# 715-166-151; RRID: AB_2340817
Donkey anti-mouse IgG conjugated to Cy2	Jackson ImmunoResearch	Cat# 103-545-155; RRID: AB_2337390
Critical commercial assays		
TRITC-labeled phalloidin	Sigma	Cat#FAK100
DAPI	Sigma	Cat#D9542
MitoTracker Deep Red	YEASEN	Cat#40734ES50
ATP Assay Kit	Beyotime	Cat#S0026
RNA-easy Isolation Reagent	Vazyme	Cat#R701-01
Rotenone	Sigma	Cat#83-79-4
PrimerScriptRT reagent Kit with gDNA Eraser	Takara	Cat#RR047A
SYBR Premix Ex Taq	Takara	Cat#RR420A
Chemiluminescent detection kit	GE healthcare	Cat#RPN2134
Experimental models: Cell lines		
D. melanogaster: Cell line S2	Laboratory of Yun Zhao	N/A
Mus. Cell line C2C12	Laboratory of Geng Liu	N/A
Experimental models: Organisms/strains		
D. melanogaster: UAS-*dMterf4* RNAi	National Institute of Genetics (NIG)	15390R-2
D. melanogaster: UAS-*dMrps23* RNAi	NIG-Fly	31842R-3
D. melanogaster: UAS-*Dref* RNAi	NIG-Fly	5838R-2
D. melanogaster: UAS-*mtSSB* RNAi	NIG-Fly	4337R-1
D. melanogaster: UAS-*Dredd* RNAi	NIG-Fly	7486R-2
D. melanogaster: UAS-*Sting* RNAi	NIG-Fly	1667R-3
D. melanogaster: UAS-*Phb1* RNAi	NIG-Fly	10691R-1
D. melanogaster: UAS-*Med8* RNAi	Vienna *Drosophila* Resource Center (VDRC)	VDRC_107783
D. melanogaster: UAS-*Tfb4* RNAi	VDRC	VDRC_101309
D. melanogaster: UAS-*PolG2* RNAi	VDRC	VDRC_30483
D. melanogaster: UAS-*mtDNA-helicsae* RNAi	VDRC	VDRC_108644
D. melanogaster: UAS-*cGlr1* RNAi	VDRC	VDRC 17112
D. melanogaster: UAS-*dSNX9* RNAi	VDRC	VDRC 105886
D. melanogaster: UAS-*Pink1* RNAi	VDRC	VDRC 109614
D. melanogaster: UAS-*Parkin* RNAi	VDRC	VDRC 104363
D. melanogaster: UAS-*Porin* RNAi	VDRC	VDRC 101336
D. melanogaster: UAS-*Debcl* RNAi	VDRC	VDRC 47515
D. melanogaster: UAS-*sesB* RNAi	VDRC	VDRC 104576

(Continued on next page)

Continued

REAGENT or RESOURCE	SOURCE	IDENTIFIER
D. melanogaster: UAS-*Rel* RNAi	Tsing Hua Fly Center (THFC)	THU 4885
D. melanogaster: UAS-*PolrMT* RNAi	THFC	THU 1689
D. melanogaster: UAS-*Buffy* RNAi	Bloomington *Drosophila* Stock Center (BDSC)	BDSC 29608
D. melanogaster: Mef2-GAL4	BDSC	BDSC 27390
D. melanogaster: TH-GAL4	BDSC	BDSC 8848
D. melanogaster: UAS-HA-dMterf4	This paper	N/A
D. melanogaster: UAS-HA-MTERF4	This paper	N/A
D. melanogaster: UAS-HA-dMrps23	This paper	N/A
D. melanogaster: UAS-HA-MRPS23	This paper	N/A
D. melanogaster: UAS-Flag-Med8	This paper	N/A
D. melanogaster: UAS-HA-Med8	This paper	N/A
D. melanogaster: UAS-HA-MED8	This paper	N/A
D. melanogaster: UAS-Flag-Tfb4	This paper	N/A
D. melanogaster: UAS-HA-Tfb4	This paper	N/A
D. melanogaster: UAS-Tfb4-HA	This paper	N/A
D. melanogaster: UAS-Flag-GTF2H3	This paper	N/A
D. melanogaster: UAS-mtSSB-HA	This paper	N/A
D. melanogaster: UAS- mtSSBΔ1-47-HA	This paper	N/A
D. melanogaster: UAS- mtSSBΔ1–47/85-91-HA	This paper	N/A
D. melanogaster: UAS-PolG2-HA	This paper	N/A
D. melanogaster: UAS-Tom20(1–50)-PolG2Δ1-20-HA	This paper	N/A
D. melanogaster: UAS-Tom20(1–50)-PolG2Δ1-20-G31E-HA	This paper	N/A
D. melanogaster: UAS-mtDNA-helicase-HA	This paper	N/A
D. melanogaster: UAS-Tom20(1–50)-mtDNA-helicaseΔ1-33-HA	This paper	N/A
D. melanogaster: UAS-Tom20(1–50)-mtDNA-helicaseΔ1-33-A442P-HA	This paper	N/A
D. melanogaster: UAS-Rel-HA	This paper	N/A
D. melanogaster: UAS- RelΔ152-334-HA	This paper	N/A
Software and algorithms		
FV10-ASW 4.2 Viewer	Olympus	https://www.olympus-lifescience.com
GraphPad Prism	GraphPad	https://www.graphpad.com

RESOURCE AVAILABILITY

Lead contact

Further information and requests for resources should be directed to and will be fulfilled by the lead contact, Qing Zhang (zhangqing@nju.edu.cn).

Materials availability

This study did not generate new unique reagents.

Data and code availability

- The data reported in this paper will be shared upon request to the lead corresponding author (zhangqing@nju.edu.cn).
- This paper does not report original code.
- Any additional information required to reanalyze the data reported in this paper is available from the lead contact upon request.

EXPERIMENTAL MODEL AND STUDY PARTICIPANT DETAILS

Drosophila genetics

Fly culture and crosses were performed using standard fly food containing yeast, cornmeal, and molasses, and the flies were raised at 25°C. The *w1118* line was used as a wild-type genetic background. The transgenic flies in this paper were generated by microinjection of pUAST vector-cloned genes into *w1118* embryos. All flies used in the experiments contained both males and females. Except for experiments related to lifespan, all the flies used in other experiments were approximately 2-day-old.

Cell culture and transfection

S2 cells were maintained at 25°C in Schneider's *Drosophila* medium (Sigma, S9895) supplemented with 10% FBS (Gibco, F0718), 100 U/ml penicillin (Life Technologies), and 100 μg/ml streptomycin (Life Technologies). Transfection of S2 cells was performed using PEI according to the manufacturer's instructions (Sigma).

C2C12 cells were cultured in a 37°C incubator 5% CO2 in Dulbecco's modified Eagle's medium (Gibco, 12800-058) supplemented with 10% FBS (Gibco, F0718), 100 U/ml penicillin (Life Technologies) and 100 μg/ml streptomycin (Life Technologies).

METHOD DETAILS

Climbing assay

The climbing ability assays were conducted as previous reported.[55] Groups of 2-day-old 50 flies were transferred into 1.25cm diameter and 28 cm high glass tubes for 30 min incubation at room temperature for environmental acclimatization. Then the flies were tapped to the bottom of the tubes, and measured the number of flies that can climb above the 5-cm mark by 10s after the tap. Five trials were performed for each group, allowing for 1-min rest period between each trial. Five different groups were analyzed for each genotype.

Lifespan analysis

Groups of 25 1-day-old flies were placed into separate tubes with food and were maintained at 25°C. The flies were transferred to tubes with fresh food every 2–3 days, and the number of dead flies was counted. In these experiments, a minimum of 100 flies were tested for each genotype. Data were presented as Kaplan-Meier survival distributions, and significance was determined by log rank tests.

ATP assay

ATP concentrations were assessed using the ATP Assay Kit (Beyotime, S0026). Five thoraces of 2-day-old flies were homogenized in cell lysis reagent in ATP assay kit. Luminescence was measured by Infine M200 Pro (Tecan, Swiss), and the results were compared to standards.

Immunohistochemistry

For fly tissues, thoraces were dissected from adult flies and fixed in 4% paraformaldehyde (PFA) in phosphate-buffer saline (PBS) for 30 min and washed 3 times in 0.1% PBST (PBS + Triton X-100) for 20 min. Primary antibodies were diluted 1:200 in PBST and incubated overnight at 4 °C. The primary antibodies used were: mouse anti-ATP5A, mouse anti-HA. Samples were washed 3 times in PBST and incubated with the secondary antibodies for 2h at room temperature. The secondary antibodies used were: anti-mouse Alexa Fluor 488; anti-mouse Alexa Fluor 555; DAPI and phalloidin. Then samples were rinsed 3 times with PBST for 20 min and mounted in 60% glycerol and imaged by FV10-ASW Olympus confocal microscope.

For S2 cells, 48h after transfected, cells were harvested and washed with PBS. Cells were fixed in 4% paraformaldehyde for 15 min, permeabilized with PBST for 15 min, washed with PBS 3 times for 10 min. To mark the nucleus, cell membrane and mitochondria, cells were stained with DAPI, phalloidin and Mitotracker Deep Red, respectively.

RNA extraction and quantitative RT-PCR

Total RNA was extracted from flies by RNA-easy Isolation Reagent according to manufacturer's protocol and reversely transcribed by PrimeScriptRT reagent Kit with gDNA Eraser. PCR was performed using SYBR Premix Ex Taq and an Applied Biosystems 7500 Real-time PCR system. Relative mRNA levels were calculated by normalizing against the endogenous *Act5C* mRNA levels (internal control). For each experiment, qPCR reactions were performed in triplicate. Primer sequences used in this study were described in Table S1.

Western blot and immunoprecipitation

Samples were collected and lysates were separated by SDS-PAGE using standard procedures and transferred onto a PVDF membrane. The membrane was blocked with 5% non-fat milk in TBST buffer and incubated with primary antibodies overnight at 4°C. The membrane was washed and incubated in HRP labeled secondary antibodies for 2h at room temperature. For the IP experiments, cells were lysed and the cell lysates were incubated with antibody for 2 h at 4°C. After adding 20ul A/G agarose beads, then the cell lysates were incubated for 1 h at 4°C. The immuno-precipitates were washed three times and centrifuged at 2500 rpm at 4°C. Then the immuno-complexes were extracted by boiling in loading buffer for 5 min, and detected through western blot.[56]

Relative cytosolic mtDNA copy number measurement

To get mitochondria-depleted fraction, fifty thoraces were washed, resuspended in ice-cold hypotonic buffer (300 mM Sucrose, 10 mM Na-HEPES, 0.2 mM EDTA, pH 7.2) and then lysed by Dounce homogenization. The lysates were centrifuged at 600x g twice for 15 min at 4 °C to remove cell debris, the supernatants were centrifuged at 8000x g for 15 min at 4 °C to pellet mitochondria, then the supernatants were further purified for analysis of relative cytosolic mtDNA levels with quantitative real-time PCR.[57,58] Pool each step pellets for the corresponding nuclear DNA (nDNA) extracts. The relative cytosolic mtDNA copy number levels were determined by the ratios of mtDNA/nDNA. The mitochondrial *16S rRNA* gene and the nuclear DNA *Rpl32* gene were used to measure the mtDNA and nDNA, respectively. Quantitative PCR using primers for the mitochondrial *16S rRNA* gene and the nuclear *RpL32* gene were described in Table S1.

For mouse (Mus) C2C12 cells, the mitochondrial *16S rRNA* gene (for Figure S7) or ND1 gene (for Figures 3J–3L) and the nuclear *HK2* gene were used to measure the mtDNA and nDNA, respectively. Quantitative PCR primers for the mitochondrial *16S rRNA* gene and the nuclear *HK2* gene were described in Table S1.

The QPCR and PCR primers for *ND1* gene used to specifically detect the Mus C2C12 mtDNA in *Drosophila* mitochondria-depleted cytosolic extracts were described in Table S1.

QUANTIFICATION AND STATISTICS ANALYSIS

Statistics

GraphPad Prism8 was used to perform the statistical analysis and graphical display of data. Significance is expressed as p values which was determined with two tailed, unpaired, parametric or nonparametric tests as indicated in figure legends. For two group comparisons, unpaired t-test was used, and the Student's *t* test was used for the analysis of three or more independent experiments. For comparison of survival curves, Log rank (Mantel Cox) test was used, $p < 0.05$ was considered significant. *, $p < 0.05$; **, $p < 0.01$; ***, $p < 0.001$; ****, $p < 0.0001$.